OPEN ACCESS

University of BRISTOL

Habibi, M., Vahidinasab, V., Sepasian, M. S., Allahham, A., Giaouris, D., Taylor, P., & Aghaei, J. (2021). Stochastic Procurement of Fast Reserve Services in Renewable Integrated Power Systems. *IEEE Access*, *9*, 30946-30959. [9352722]. https://doi.org/10.1109/ACCESS.2021.3058774

Publisher's PDF, also known as Version of record

License (if available):
CC BY-NC-ND

Link to published version (if available):
10.1109/ACCESS.2021.3058774

Link to publication record in Explore Bristol Research
PDF-document

This is the final published version of the article (version of record). It first appeared online via IEEE at https://doi.org/10.1109/ACCESS.2021.3058774 .Please refer to any applicable terms of use of the publisher.

University of Bristol - Explore Bristol Research
General rights

This document is made available in accordance with publisher policies. Please cite only the published version using the reference above. Full terms of use are available:
http://www.bristol.ac.uk/red/research-policy/pure/user-guides/ebr-terms/

IEEE Access
Multidisciplinary | Rapid Review | Open Access Journal

Received January 16, 2021, accepted February 5, 2021, date of publication February 11, 2021, date of current version February 26, 2021.

Digital Object Identifier 10.1109/ACCESS.2021.3058774

Stochastic Procurement of Fast Reserve Services in Renewable Integrated Power Systems

MAHDI HABIBI[1], VAHID VAHIDINASAB[1,2], (Senior Member, IEEE), MOHAMMAD SADEGH SEPASIAN[1], ADIB ALLAHHAM[2], DAMIAN GIAOURIS[2], PHIL TAYLOR[3], (Senior Member, IEEE), AND JAMSHID AGHAEI[4], (Senior Member, IEEE)

[1]Faculty of Electrical Engineering, Shahid Beheshti University, Tehran 19839 69411, Iran
[2]School of Engineering, Newcastle University, Newcastle upon Tyne NE1 7RU, U.K.
[3]Faculty of Engineering, University of Bristol, Bristol, BS8 1QU, U.K.
[4]School of Energy Systems, Lappeenranta-Lahti University of Technology (LUT), 53850 Lappeenranta, Finland

Corresponding author: Jamshid Aghaei (jamshid.aghaei@lut.fi)

ABSTRACT Ensuring the security and quality of supply in a power system after a contingency event is one of the most challenging tasks for an electricity system operator. This work is initiated by this challenge and proposes a solution based on the use of provided reserves by fast generators, storage devices, and wind farms. A coordinated model is proposed in a joint energy and reserves market considering their corresponding cost to ensure the adequacy in the simultaneous deployment of reserves for the different sources of uncertainties. The Benders decomposition approach is used in the modeling of the stochastic security-constrained unit commitment, and considering the large-scale and complex nature of the model, acceleration techniques are suggested to reduce the execution time. The proposed model is tested on the 6-bus and the IEEE 118-bus test systems. Numerical results show that the optimal values of reserves successfully address contingencies in both of the critical and normal periods after the contingencies and the optimal solution is calculated in a reasonable computing time.

INDEX TERMS Critical period, post-contingency actions, stochastic security-constrained unit commitment, reserve services, benders decomposition, energy storage, wind power fluctuations.

INDICES & SETS

b	Index of segments of piece-wise function.
B	Index of the base case (base scenario).
s	Index of buses.
l	Index of transmission lines.
ch/dis	Indices of charging/discharging of storage.
c	Index of contingencies.
t	Index of time.
δ	Index of scenarios of uncertainty.
i	Index of generators.
m	Index of storage devices.
n	Index of wind farms.
U/D	Indices of upward/downward re-dispatches.
1, 2, 3	Indices of reserves in different types.
τ_1, τ_2	Indices of critical period and post-contingency.
Λ	Set of generators connected to bus s.
ϕ	Set of storage devices connected to bus s.
ψ	Set of wind farms connected to bus s.

PARAMETERS

FOR_l	Forced outage rate of transmission lines.
Pl_s^t	Active power of demands [MW].
$ILOI_l^t$	Index of line outage impact factor.
γ	Emergency rating of transmission lines.
ERu_i	Emergency ramp up of generators [MW/h].
ERu_i	Emergency ramp down of generators [MW/h].
Qc_i	Type-1 FRS rating of generators [%].
Qr_i	Type-2 FRS rating of generators [%].
Ru_i, Rd_i	Ramp up/down limits of generator [MW/h].
RSu_i	Shut-down ramp rate of generator [MW/h].
RSd_i	Start-up ramp rate of generator [MW/h].
$SC_i DC_i$	Start-up, shut-down costs of generators [$].
NC_i	Fixed costs of generators [$/h].

The associate editor coordinating the review of this manuscript and approving it for publication was Fabio Massaro.

This work is licensed under a Creative Commons Attribution-NonCommercial-NoDerivatives 4.0 License.
For more information, see https://creativecommons.org/licenses/by-nc-nd/4.0/

$T_s^{l,B}$ Shift of lines' power flow due to change of injection at bus s in the base case.
$T_s^{l,c}$ Shift of lines' power flow due to change of injection at bus s in contingencies.
$\zeta 1^t$, $\zeta 2^t$ Normalized cost multipliers of time-steps.
Ω_δ Probability of scenarios [%].
η_m^{ch} Efficiency of storage charging [%].
η_m^{dis} Efficiency of storage discharging [%].
λ_i^b Production cost of generators [$/MWh].
λ_m^{dis} Cost of storage discharge [$/MWh].
$\lambda_m^{ch,(U/D)}$ Reserve upward/downward cost in storage charging mode [$/MW].
$\lambda_m^{dis,(U/D)}$ Reserve upward/downward cost in storage discharging mode [$/MW].
λ_n^D Reserves cost of wind farms [$/MW].
$\lambda_i^{1,(U/D)}$ Cost of Type-1 reserve of generators [$/MW].
$\lambda_i^{2,(U/D)}$ Cost of Type-2 reserve of generators [$/MW].
$\lambda_i^{3,(U/D)}$ Cost of Type-3 reserve of generators [$/MW].
α Acceptable wind curtailment percent [%].
β_n^1, β_n^2 Wind farm participation rate in reserve deployment of Type-1 and Type-2 [%].
$\Delta t1$, $\Delta t2$ Time steps of operation/critical period [h].

VARIABLES

$E_{m,t}^B$ Energy of storage in base case [MWh].
$E_{m,t}^c$ Energy of storage in contingencies [MWh].
FG_t Total energy cost of generators [$].
FS_t Total energy cost of storage devices [$].
FRG_t Total reserve cost of generators [$].
FRS_t Total reserve cost of storage devices [$].
FRW_t Total reserve cost of wind farms [$].
Fl_l^t Power flow of transmission lines [MW].
$I_{i,t}$ Generator on/off binary variable.
$J_{m,t}$ Storage discharging status in base case.
$J_{m,t}^c$ Storage discharging status in contingencies.
$P_{i,t}$ Base dispatches of generators [MW].
$P_{i,t}^\delta$ Dispatch of generators in scenarios [MW].
$P_{m,t}^{ch}$ Dispatch of storage in charge mode [MW].
$P_{m,t}^{dis}$ Dispatch of storage in discharge mode [MW].
$P_{n,t}^\delta$ Dispatch of wind farms in scenarios [MW].
$r_{i,t}^{(U/D),\delta}$ Reserve realization in wind scenarios [MW].
$R_{m,t}^{ch,(U/D)}$ Reserves of storage in charging mode [MW].
$R_{m,t}^{dis,(U/D)}$ Reserves of storage in discharge mode [MW].
$R_{i,t}^{1,(U/D)}$ Type-1 FRSs provided by generators [MW].
$R_{i,t}^{2,(U/D)}$ Type-2 FRSs provided by generators [MW].
$R_{i,t}^{3,(U/D)}$ Type-3 regular reserves of generators [MW].
$R_{n,t}^{1,D}$ Type-1 FRSs provided by wind farms [MW].
$R_{n,t}^{2,D}$ Type-2 FRSs provided by wind farms [MW].
S_B^t Slack variable of load curtailment in base case sub-problem [MW].
$S_c^{t,\tau}1$ Slack variable of load curtailment in sub-problem 2 [MW].
$S_c^{t,\tau}2$ Slack variable of load curtailment in sub-problem 3 [MW].
$S1_c^t$, $S2_c^t$, $S3_c^t$ Slack variables of load curtailment in sub-problems 2 and 3 [MW].
$st_{i,t}$, $sd_{i,t}$ Binary variables for start-up and shut-down statuses.
$T_{i,t}^{\text{on}}$, $T_{i,t}^{\text{off}}$ On/off duration time of generators [h].
μ Dual variables of different sub-problems.

I. INTRODUCTION

Maintaining the balance between demand and generation is one of the highest priorities of power system operators [1], [2]. This balance can be disturbed with increasing penetration of renewable sources, which has intermittent outputs, and the occurrence of contingency events [3], [4] which the Friday 9 August 2019 power outage of the UK is the recent example of this issue [5]. To restore the balance between supply and demand and to prevent cascading failures in the power system, reserves must be dispatched very fast.

A. AIM AND MOTIVATION

There are various types of balancing services, including the frequency and reserve services that are available for regulation and contingency management purposes [6]. In [7] a complete list of services procured by the UK National Grid Energy Systems Operator (ESO) for balancing demand and supply across Britain's transmission system is provided. In normal operation condition, the regulation reserves adjust the imbalance of demand and generation, caused by the variation of load and renewable generation [8], [9]. The contingency reserves are provided through both of the fast and slow-responding reserve units. The ability of these units to secure the power system is usually checked using the *N-1* or *N-K* Contingency Analysis (CA).

B. LITERATURE SURVEY

The unit commitment problem considers the day-ahead scheduling of power system [10], [11]. Recently, scheduling contingency reserves have attracted considerable attention from researchers. The optimal load shedding in [12] and the demand response in [13] are included by the Security-Constrained Unit Commitment (SCUC) problem; however, the response time of reserves is not considered in [13]. A two-stage robust model is presented in [14] to consider the *N-K* outages of lines and generators. A mixed day-ahead and intraday min-max model is presented in [15], where control actions are planned to prevent a cascading failure. In [16], a contingency-constrained unit commitment is presented to schedule the reserve units in case of line/unit outages.

Scheduling generators that provide Fast Reserve Services (FRSs) in the day-ahead market is presented in [17] and [18] to secure the system directly after the occurrence of a contingency event. In [18], the re-dispatch of units formulated as a SCUC problem, and the units are planned to intervene in two different periods after the occurrence of a contingency event. The reserves of the first period (critical duration) are used to secure the system immediately after the occurrence of the contingency event, and the reserves of the second period aim to secure the system, 10 minutes after the occurrence of a contingency event. The reserves of both intervals cannot work cooperatively during the same period.

On the other hand, the joint scheduling of contingency and regulation reserves are also considered in the literature. The uncertainty associated with the use of renewable energy sources is considered either within a robust model or a stochastic model with a limited number of scenarios [6], [19]. In [20], a robust-stochastic model is presented. That model aims to find a feasible solution for at least one scenario, but not for the base operation point, which is not suitable for real-world cases. This is one of the issues that is considered in our model in this paper by adding a sub-problem corresponding to the base case. Here, the ''base case'' indicates the operational decision variable in the stochastic problem, which is usually scheduled based on the expected values of uncertainty variables. In [21], the regulation and contingency reserves are scheduled jointly for a distribution network, using a decomposed robust SCUC model. That model considers the critical lines to be protected against outages to increase the reliability of the system. The model developed in this paper also considers the high impact outages for ranking *N-1* to prevent dangerous contingencies. Both models presented in [20] and [21] do not consider the response time of units or contingencies, which is considered in this paper. A multi-resolution robust SCUC is also presented in [22], which copes with the uncertainties of demand and the intermittency of renewable energy sources. That model can deal efficiently with the small networks but not with the large ones, and this is due to the huge computation cost. Reference [23] suggests a two-stage stochastic SCUC for planning the wind energy and conventional units in the day-ahead market with *N-1* contingencies. This model considers all the scenarios in *N-1* contingency, which burdens the solutions and leads to a large computation cost. In [24], the presented stochastic model considers the uncertainties of generators and load, and also branch contingencies. The generated scenarios are based on the Forced Outage Rate (FOR) of the components. The model is also not decomposed, and hence, it is not suitable for large scale networks. In addition, the response time and critical duration are not considered in the model.

C. RESEARCH GAP

According to the aforementioned literature review, it can be seen that there is no comprehensive model that able to schedule the regulation and slow/fast-responding contingency reserves considering the stochastic behavior of renewable energy sources, the response time of different facilities and contingencies, and provide the solution for the base case and all the important scenarios. This paper addresses this research gap by developing a comprehensive model. Different types of reserve providers are considered in this model to meet the dynamic response required in each case.

Moreover, this work advances the state-of-the-art by providing an exhaustive model that is able to concurrently coordinate the regulation and contingency reserves and also dispatch the appropriate reserves among the conventional generators, generators providing FRSs, and the storage facilities. As these units provide different response times, the model is able to select the necessary reserves according to the dynamic response required to restore the demand and generation balance.

D. CONTRIBUTIONS

This paper presents a stochastic SCUC model considering the reserves provided by conventional generators, generators with FRSs, and storage facilities. Two types of generators can deploy the FRSs: the first type deploys very fast services that can be used for immediate re-dispatches, and the second type provides fast enough reactions which can be used as regulation reserves. The response time of these services can deal with the dynamics of different phenomena considered in the model. The model optimizes jointly the operational cost and the cost of reserves considered explicitly in the model. In this paper, the model coordinates the operation of generators with FRSs such that: (i) The first type of generators with FRSs is used to provide balancing service with immediate response and during a short period after the contingency event occurrence. Also, both types of generators with FRSs are used for regulation reserves; (ii) The conventional generators, as well as generators with FRSs, are used to provide reserves for stable re-dispatch after the contingency occurrence.

Solving an exhaustive model can be complex and requires a long computational time. For that, a decomposition method based on the Benders algorithm and the Aggregation of Sub-Problems (ASP) is proposed. The purpose of this method is to reduce the solution time of the exhaustive model. This ASP method solves one aggregated problem instead of solving sub-problems for each time/scenario, usually used in the literature. The consideration of all possible cases in *N-1* contingency requires a long computation time; consequently, it will burden the model. On the other hand, generating predefined scenarios for outages, such as presented in [23], [24] might ignore some important outage scenarios. For this reason, the Online Contingency Ranking (OCR) of overhead lines is used to evaluate the contingency events in this paper. Also, Emergency Line Rating (ELR) is considered to reduce the total cost.

In brief, the main contributions of this paper are summarized as follows:

- Develop a model to schedule the regulation and contingency reserves while considering the stochastic nature of wind energy, the response time of different facilities

and contingencies, and provide the solution for the base case and all the important scenarios;
- Coordinate different performances of generators including the performance as contingency reserve provider and the performance as regulation reserves;
- Develop a solving technique to accelerate the calculation time. This technique is based on the online contingency ranking method and the aggregation of subproblems resulting from the application of Benders decomposition.

The remainder of this paper is arranged as follows. Sections II and III illustrate the problem formulation and the solving technique. The results of two different case studies are discussed in Section IV. In Section V, the conclusion is outlined.

II. STOCHASTIC PROCUREMENT OF FAST RESERVE SERVICES

A. METHOD OF SCENARIO GENERATION

In this paper, wind farms are considered in the model and scenario generation; however, other types of renewable energy sources can be considered in the same way. The scenarios of wind speed are calculated based on the Weibull distribution. A large number of random samples are firstly generated around the mean value of predicted wind speed, which, in turn, is based on meteorological data [25]. Then, a reduction method based on Kantorovich distance (so-called probability distance method) is used to measure the similarity and reduce the number of scenarios [26]. The output energy of wind farms is calculated based on the power curve of turbines.

B. MODEL OF THE STOCHASTIC SCUC

The objective function of the stochastic SCUC model consists of the weighted sum of the operational cost and the lost opportunity cost for the different scenarios. In this paper, the lost opportunity cost is the penalty of downward re-dispatches of generators "$r_{i,t}^{D,\delta}$". Adding the reserve deployment cost to the conventional stochastic objective function of SCUC (2) leads to the objective function given by (1).

$$\min_{I,P_{(i/m/n)},R1,R2,R3} \sum_t FG_t + FS_t + FRG_t + FRS_t + FRW_t \tag{1}$$

$$FG_t = \Delta t1 \sum_i \Big(SC_i st_{i,t} + DC_i sd_{i,t} + NC_i I_{i,t} + \sum_\delta \Omega_\delta \zeta 1^t \big(rc_i^D r_{i,t}^{D,\delta} + \sum_b \lambda_i^b P_{i,t}^{b,\delta} \big) \Big) \tag{2}$$

$$st_{i,t} - sd_{i,t} = I_{i,t} - I_{i,(t-1)} \tag{3}$$

$$st_{i,t} \le I_{i,t'} \quad \forall t \le t' \le t + T_i^{\text{on,min}} - 1 \tag{4}$$

$$sd_{i,t} \le 1 - I_{i,t'} \quad \forall t \le t' \le t + T_i^{\text{off,min}} - 1 \tag{5}$$

$$P_{i,t} - P_{i,(t-1)} \le Ru_i I_{i,t} + RSu_i st_{i,t} \tag{6}$$

$$P_{i,(t-1)} - P_{i,t} \le Rd_i I_{i,t} + RSd_i sd_{i,t} \tag{7}$$

$$P_i^{\min} I_{i,t} \le \Big(P_{i,t}^\delta = \sum_b P_{i,t}^{b,\delta} \Big) \tag{8}$$

$$P_{i,t}^{b,\delta} \le P_i^{b,\max} I_{i,t} \tag{9}$$

$$\sum_i P_{i,t} + \sum_m P_{m,t} + \sum_\delta \Omega_\delta \sum_n P_{n,t}^\delta = \sum_s Pl_s^t \tag{10}$$

$$\sum_i P_{i,t}^\delta + \sum_m P_{m,t} + \sum_n P_{n,t}^\delta = \sum_s Pl_s^t. \tag{11}$$

The terms FS_t, FRG_t, FRS_t, and FRW_t in (1) are given respectively in (12), (19), (37), and (44), and are explained later in this section. In addition, different periods are considered in the cost functions. The $\Delta t1$, which is $1h$ (60 minutes), is the operation time-step, and $\Delta t2$, which is $\frac{1}{6}h$ (10 minutes), is the required time for stable re-dispatches after contingencies. Constraint (3) shows the relationship between binary variables of start-up, shut-down, and the variable of on/off status. The minimum on/off periods of generators are considered by (4) and (5). The ramp rate limits are controlled by (6) and (7). The equations of generator piece-wise steps and the production limits are presented by (8) and (9). The load balance constraints are given by (10) and (11).

C. MODEL OF STORAGE DEVICES

In this paper, the cost of energy purchasing is the cost paid to the generators to charge the storage devices; consequently, it is included implicitly in the cost function given by (2), while the profit of energy storage devices is represented by (12). The operation of the energy storage devices and their constraints are given by (13)–(19). E_{m,t_0} is the initial value of the stored energy of storage devices. Constraint (13) is the relation between charging/discharging and the stored energy of the storage devices. The energy limits of storage devices are constrained by (14). Constraint (15) ensures that the storage devices have enough energy to be involved in the energy market in the next day. Also, the limits of charging/discharging and the dispatched energy of them are given by (16)–(18).

$$FS_t = \Delta t1 \zeta 2^t \sum_m \lambda_m^{dis} P_{m,t}^{dis} \tag{12}$$

$$E_{m,t}^B = E_{m,(t-1)}^B + \Delta t1 \Big(P_{m,t}^{ch} \eta_m^{ch} - P_{m,t}^{dis} / \eta_m^{dis} \Big) \tag{13}$$

$$E_{m,t}^{\min} \le E_{m,t}^B \le E_{m,t}^{\max} \tag{14}$$

$$E_{m,t_0}^B = E_{m,t_{24}}^B \tag{15}$$

$$P_{m,t}^{dis} \le J_{m,t} P_m^{dis,\max} \tag{16}$$

$$P_{m,t}^{ch} \le (1 - J_{m,t}) P_m^{ch,\max} \tag{17}$$

$$P_{m,t} = P_{m,t}^{dis} - P_{m,t}^{ch}. \tag{18}$$

D. MODEL OF RESERVE DEPLOYMENT

The model presented in this paper classifies the reserve units into three types. Type-1 includes the reserve units to be used immediately after the occurrence of a contingency event. The reserve units to be used to stabilize the system at a new operation point after the first minutes are indicated by Type-2. This period is called the critical period. The period after Type-2 units intervention is called the post-contingency period. The reserve units, which are used to regulate the system and to

address the variations of wind generation, are classified as Type-3. In the following, the deployment model of the reserve units of types 1, 2, and 3 are presented.

1) DEPLOYMENT MODEL OF GENERATORS

As stated, the conventional generators and generators with FRSs are providing upward/downward reserves and represent the main resource of system flexibility. The cost of reserves provided by these generators is given by (19). In this equation, the reserves deployed from the units Type-1, Type-2, and Type-3 are indicated respectively by R^1, R^2, and R^3. The first type of generators with FRSs (immediate response) provides up to $Qc_i\%$ of emergency ramp rate, and the corresponding limits in upward and downward are presented by (20)–(23). The conventional generators show a slow response for dispatching the required energy. The limits of their contribution in providing reserves are given by (24)–(27). The second type of generators with FRSs provides up to $Qr_i\%$ of emergency ramp rate, and they will be used to restore the imbalance resulting from the fluctuation of wind energy by regulation reserves. The corresponding constraints are given by (28)–(32).

$$FRG_t = \zeta 1^t \sum_i \Big(\big(\lambda_i^{1,U} R_{i,t}^{1,U} + \lambda_i^{1,D} R_{i,t}^{1,D}\big) + \big(\lambda_i^{2,U} R_{i,t}^{2,U} + \lambda_i^{2,D} R_{i,t}^{2,D}\big) + \big(\lambda_i^{3,U} R_{i,t}^{3,U} + \lambda_i^{3,D} R_{i,t}^{3,D}\big) \Big) \tag{19}$$

$$R_{i,t}^{1,U} \le Qc_i ERu_i I_{i,t} \tag{20}$$

$$R_{i,t}^{1,D} \le Qc_i ERd_i I_{i,t} \tag{21}$$

$$P_{i,t} + R_{i,t}^{1,U} \le P_i^{\max} I_{i,t} \tag{22}$$

$$P_{i,t} - R_{i,t}^{1,D} \ge P_i^{\min} I_{i,t} \tag{23}$$

$$R_{i,t}^{2,U} \le ERu_i I_{i,t} \tag{24}$$

$$R_{i,t}^{2,D} \le ERd_i I_{i,t} \tag{25}$$

$$P_{i,t} + R_{i,t}^{2,U} \le P_i^{\max} I_{i,t} \tag{26}$$

$$P_{i,t} - R_{i,t}^{2,D} \ge P_i^{\min} I_{i,t} \tag{27}$$

$$P_{i,t}^{\delta} = P_{i,t} + r_{i,t}^{U,\delta} - r_{i,t}^{D,\delta} \tag{28}$$

$$r_{i,t}^{U,\delta} \le Qr_i ERu_i I_{i,t} \tag{29}$$

$$r_{i,t}^{D,\delta} \le Qr_i ERd_i I_{i,t} \tag{30}$$

$$R_{i,t}^{3,U} \ge r_{i,t}^{U,\delta} \tag{31}$$

$$R_{i,t}^{3,D} \ge r_{i,t}^{D,\delta}. \tag{32}$$

The first type of generators with FRSs can be used during the critical and post-contingency periods, and they can also be used to provide regulation reserves. Also, the second type of generators with FRSs can be used in post-contingency and as regulation reserves. Hence, it is important to coordinate the participation of these generators, as shown by (33)–(36).

$$R_{i,t}^{1,U} + R_{i,t}^{3,U} \le ERu_i I_{i,t} \tag{33}$$

$$R_{i,t}^{2,U} + R_{i,t}^{3,U} \le ERu_i I_{i,t} \tag{34}$$

$$R_{i,t}^{1,D} + R_{i,t}^{3,D} \le ERd_i I_{i,t} \tag{35}$$

$$R_{i,t}^{2,D} + R_{i,t}^{3,D} \le ERd_i I_{i,t}. \tag{36}$$

2) DEPLOYMENT MODEL OF STORAGE DEVICES

The energy supplied by the storage devices depends on their available stored energy. In normal operation conditions, the storage devices exchange the energy with the grid according to a fixed schedule. However, providing energy from the storage devices during the post-contingency period may deplete all of their stored energy; consequently, the storage devices will not be able to provide energy during the critical period. On the other hand, the operator of storage devices can recover their stored energy with real-time decisions. The cost of energy deployment from storage devices consists of the upward and downward reserves in two modes: charging and discharging, as shown by (37). Equations (40)–(43) show that the stored energy of storage devices and the power exchanged with the grid during the charging and discharging should remain within limits.

$$FRS_t = \zeta 2^t \sum_m \Big(\lambda_m^{dis,U} R_{m,t}^{dis,U} + \lambda_m^{dis,D} R_{m,t}^{dis,D} + \lambda_m^{ch,U} R_{m,t}^{ch,U} + \lambda_m^{ch,D} R_{m,t}^{ch,D} \Big) \tag{37}$$

$$E_{m,t}^{c} = E_{m,t}^{B} + \Delta t 2 \Big(R_{m,t}^{ch,U} \eta_m^{ch} - R_{m,t}^{dis,U} / \eta_m^{dis} \Big) \tag{38}$$

$$E_{m,t}^{\min} \le E_{m,t}^{c} \le E_{m,t}^{\max} \tag{39}$$

$$P_{m,t}^{dis} + R_{m,t}^{dis,U} \le J_{m,t} P_m^{dis,\max} \tag{40}$$

$$P_{m,t}^{ch} + R_{m,t}^{ch,U} \le (1 - J_{m,t}) P_m^{ch,\max} \tag{41}$$

$$R_{m,t}^{dis,D} \le P_{m,t}^{dis} \tag{42}$$

$$R_{m,t}^{ch,D} \le P_{m,t}^{ch}. \tag{43}$$

3) CONTROL OF WIND FARMS DURING POST-CONTINGENCY PERIOD

The cost of reserve energy deployment from the wind farms is given by (44). The wind farms do not provide upward reserves, but their power can be curtailed during the critical and post-contingency periods. The maximum reserve provided by wind farms during the post-contingency and critical periods is limited by (46) and (47). Equation (48) defines the limit for the curtailment of wind energy and shows that over $\alpha\%$ of wind power will be used.

$$FRW_t = \zeta 1^t \sum_n \lambda_n^D (R1_{n,t}^D + R2_{n,t}^D) \tag{44}$$

$$P_{n,t}^{\delta} \le P_{n,t}^{\delta,\max} \tag{45}$$

$$R_{n,t}^{1,D} \le \beta_n^1 \sum_{\delta} \Omega_\delta P_{n,t}^{\delta} \tag{46}$$

$$R_{n,t}^{2,D} \le \beta_n^2 \sum_{\delta} \Omega_\delta P_{n,t}^{\delta} \tag{47}$$

$$\sum_{\delta} \Omega_\delta (P_{n,t}^{\max} - P_{n,t}^{\delta}) \le \alpha P_{n,t}^{\max}. \tag{48}$$

III. MODEL DECOMPOSITION

A decomposition method is adopted to reduce the complexity of the proposed model. The decomposed model consists of a

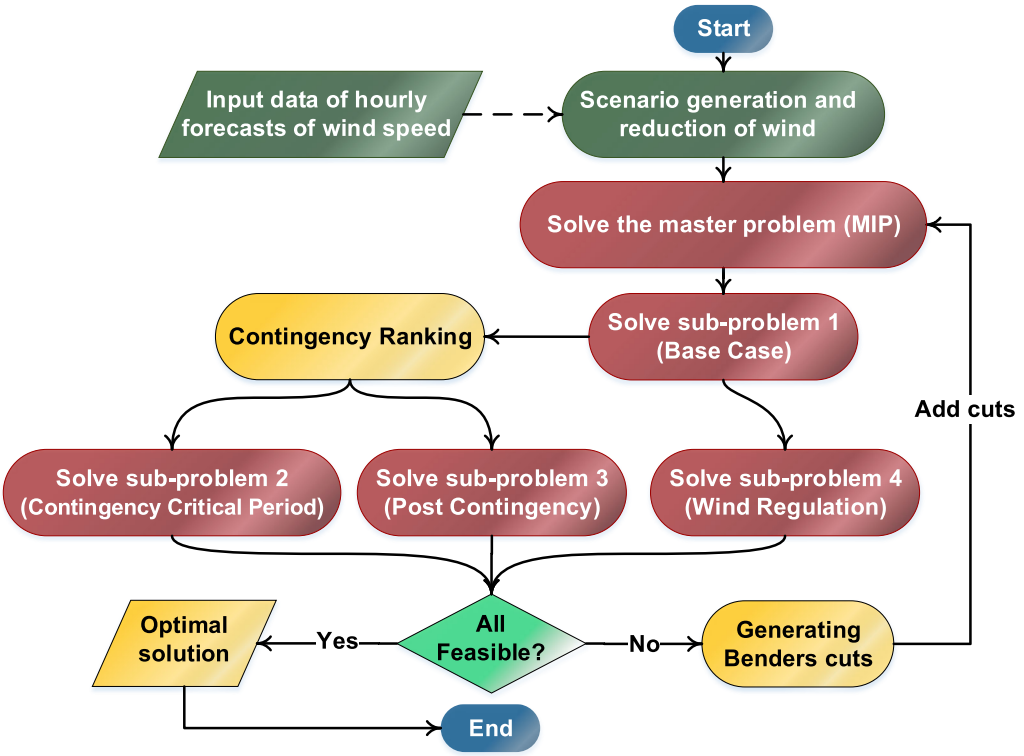

FIGURE 1. The flowchart of the proposed decompostion-based solving approach.

master problem and four sub-problems. The previous studies solve separately the sub-problems corresponding to each index: t, c, and δ [17], [18], [23]. These sub-problems are not solved until the base case is solved and no cut is generated. In this paper, an acceleration technique is developed, in which each sub-problem aggregates the sub-problems of all the indices: t, c, and δ. After that, the solving algorithm solves the master problem and all the sub-problems in the initial loop and for each iteration and generates the corresponding cuts. After that, the algorithm solves the master with new cuts, and this loop continues until no new cuts are generated. The flowchart of the proposed model is presented in Figure 1. Also, the strong cuts suggested in [27] have been used in the proposed algorithm.

A. MASTER PROBLEM

The master problem considers the total cost of stochastic SCUC given by (1), and the corresponding constraints are given by (2)–(48). The solution consists of decision variables, the schedule of power dispatching of each unit, and the reserve capacity of units that are used to solve sub-problems.

B. SUB-PROBLEM 1-BASE CASE

The objective function of this sub-problem and the corresponding constraints are given by (49)–(51). The base case checks the DC power flow for the base schedule of units, using the expected value of wind energy at normal condition. The dual variables of (50) and (51) are $\mu 1^B_{l,t}$ and $\mu 2^B_{l,t}$, respectively. The $T^{l,B}_s$ is the shift factor of lines at normal conditions based on the injected power at bus s. For each t, if the slack variable S^t_B is greater than zero, then a Benders cut will be formed according to (80).

$$\min \sum_t S^t_B \tag{49}$$

$$T^{l,B}_s\Big(\sum_{i\in\Lambda}\hat{P}_{i,t}+\sum_{m\in\phi}\hat{P}_{m,t}+\sum_{n\in\psi}\sum_{\delta}(\Omega_\delta\hat{P}^\delta_{n,t}) - Pl^t_s - S^t_B\Big) \le Fl^{\max}_l \tag{50}$$

$$T^{l,B}_s\Big(\sum_{i\in\Lambda}\hat{P}_{i,t}+\sum_{m\in\phi}\hat{P}_{m,t}+\sum_{n\in\psi}\sum_{\delta}(\Omega_\delta\hat{P}^\delta_{n,t}) - Pl^t_s + S^t_B\Big) \ge Fl^{\max}_l. \tag{51}$$

C. SUB-PROBLEM 2-SCHEDULING DURING CRITICAL PERIOD

This sub-problem evaluates the network's constraints for the master solution during the critical period. The shift factor of lines after the outages is $T^{l,c}_s$. The objective function is the sum of slack variables of curtailments as defined by (52), and the constraints defined by (53)–(66). This sub-problem contains binary variables; hence, based on the method used

in [17], the mixed-integer sub-problem is solved. After that, fixed values will be substituted, and the sub-problem will be resolved to calculate variables and dual variables. A Benders cut will be generated as defined by (81), if the S_c^{t,τ_1} is not zero for each t and c.

$$\min \sum_t \sum_c (S_c^{t,\tau_1} = S1_c^t + S2_c^t + S3_c^t) \tag{52}$$

$$P_{m,t}^c = P_{m,t}^{dis,c} - P_{m,t}^{ch,c} \tag{53}$$

$$P_{m,t}^{dis} \le J_{m,t}^c P_m^{\text{dis,max}} \tag{54}$$

$$P_{m,t}^{ch} \le (1 - J_{m,t}^c) P_m^{\text{ch,max}} \tag{55}$$

$$P_{i,t}^c - \hat{P}_{i,t} \le \hat{R}_{i,t}^{1,U} \tag{56}$$

$$\hat{P}_{i,t} - P_{i,t}^c \le \hat{R}_{i,t}^{1,D} \tag{57}$$

$$P_{m,t}^{ch,c} - \hat{P}_{m,t}^{ch} \le \hat{R}_{m,t}^{ch,U} \tag{58}$$

$$\hat{P}_{m,t}^{ch} - P_{m,t}^{ch,c} \le \hat{R}_{m,t}^{ch,D} \tag{59}$$

$$P_{m,t}^{dis,c} - \hat{P}_{m,t}^{dis} \le \hat{R}_{m,t}^{dis,U} \tag{60}$$

$$\hat{P}_{m,t}^{dis} - P_{m,t}^{dis,c} \le \hat{R}_{m,t}^{dis,D} \tag{61}$$

$$P_{n,t}^c \le \sum_\delta (\Omega_\delta \hat{P}_{n,t}^\delta) \tag{62}$$

$$\sum_\delta (\Omega_\delta \hat{P}_{n,t}^\delta) - P_{n,t}^c \le \hat{R}_{n,t}^{1,D} \tag{63}$$

$$T_s^{l,c}\Big(\sum_{i\in\Lambda} P_{i,t}^c + \sum_{m\in\phi} P_{m,t}^c + \sum_{n\in\psi} P_{n,t}^c - Pl_s^t - S1_c^t\Big) \le \gamma Fl_l^{\max} \tag{64}$$

$$T_s^{l,c}\Big(\sum_{i\in\Lambda} P_{i,t}^c + \sum_{m\in\phi} P_{m,t}^c + \sum_{n\in\psi} P_{n,t}^c - Pl_s^t + S1_c^t\Big) \ge \gamma Fl_l^{\max} \tag{65}$$

$$\sum_i P_{i,t}^c + \sum_m P_{m,t}^c + \sum_n P_{n,t}^c + S2_c^t - S3_c^t = \sum_s Pl_s^t. \tag{66}$$

The dual variables of (56) to (63) are $\mu 1_{i,t}^{c,\tau_1}$, $\mu 2_{i,t}^{c,\tau_1}$, $\mu 3_{m,t}^{c,\tau_1}$–$\mu 6_{m,t}^{c,\tau_1}$, $\mu 7_{n,t}^{c,\tau_1}$, and $\mu 8_{n,t}^{c,\tau_1}$, respectively. The possible rescheduling of generators, based on the reserves and base schedules in upward/downward are controlled by (56) and (57). The reschedule limits of storage devices in charging/discharging modes and in upward/downward are considered by (58)–(61). Also, the participation of wind farms in the critical period is considered by (62) and (63). Constraints (64) and (65) control the power flow in lines, and γ is the multiplier of ELR that considers 110% of normal conditions based on [17]. Equation (66) checks the equality of the total generation and consumption in the critical period.

D. SUB-PROBLEM 3-POST-CONTINGENCY PERIOD

This sub-problem evaluates the master solution for the stable reschedule of units during the post-contingency period. The objective function of this problem is given by (67). This sub-problem is subject to a set of constraints defined by (68)–(74). The generators can participate in providing reserve as defined by (68) and (69), and the energy of wind farms can only be curtailed as defined by (71). The power flow limits in the lines and the balance of total generation/consumption are presented by (72)–(74).

$$\min \sum_t \sum_c (S_c^{t,\tau_2} = S1_c^t + S2_c^t + S3_c^t) \tag{67}$$

$$P_{i,t}^c - \hat{P}_{i,t} \le \hat{R}_{i,t}^{2,U} \tag{68}$$

$$\hat{P}_{i,t} - P_{i,t}^c \le \hat{R}_{i,t}^{2,D} \tag{69}$$

$$P_{n,t}^c \le \sum_\delta (\Omega_\delta \hat{P}_{n,t}^\delta) \tag{70}$$

$$\sum_\delta (\Omega_\delta \hat{P}_{n,t}^\delta) - P_{n,t}^c \le \hat{R}_{n,t}^{2,D} \tag{71}$$

$$T_s^{l,c}\Big(\sum_{i\in\Lambda} P_{i,t}^c + \sum_{m\in\phi} \hat{P}_{m,t} + \sum_{n\in\psi} P_{n,t}^c - Pl_{s,t} - S1_c^t\Big) \le Fl_l^{\max} \tag{72}$$

$$T_s^{l,c}\Big(\sum_{i\in\Lambda} P_{i,t}^c + \sum_{m\in\phi} \hat{P}_{m,t} + \sum_{n\in\psi} P_{n,t}^c - Pl_{s,t} + S1_c^t\Big) \ge Fl_l^{\max} \tag{73}$$

$$\sum_i P_{i,t}^c + \sum_m \hat{P}_{m,t} + \sum_n P_{n,t}^c + S2_c^t - S3_c^t = \sum_s Pl_s^t. \tag{74}$$

Here, $\mu 1_{i,t}^{c,\tau_2}$, $\mu 2_{i,t}^{c,\tau_2}$, $\mu 3_{n,t}^{c,\tau_2}$, $\mu 4_{n,t}^{c,\tau_2}$, $\mu 5_{l,t}^{c,\tau_2}$, $\mu 6_{l,t}^{c,\tau_2}$, and $\mu 7_t^{c,\tau_2}$ are the dual variables of (68) to (74), respectively. If the load curtailment of S_c^{t,τ_2} is greater than zero in each t and c, a Benders cut as defined by (82) is added to the master problem for the next iteration.

E. SUB-PROBLEM 4-SCHEDULING THE REGULATION RESERVE

The objective function and constraints of this problem are presented by (75)–(77). This sub-problem evaluates the power flow in the different wind scenarios with considering the solution of the master problem. The flow limits of lines in different scenarios are presented by (76) and (77), and their corresponding dual variables are $\mu 1_{l,t}^\delta$ and $\mu 2_{l,t}^\delta$. The Benders cut of (83) will be generated for positive values of S_δ^t for each t and δ.

$$\min \sum_t \sum_\delta S_\delta^t \tag{75}$$

$$T_s^{l,B}\Big(\sum_{i\in\gamma} \hat{P}_{i,t}^\delta + \sum_{m\in\phi} \hat{P}_{m,t} + \sum_{n\in\psi} \hat{P}_{n,t}^\delta - Pl_s^t - S_\delta^t\Big) \le Fl_l^{\max} \tag{76}$$

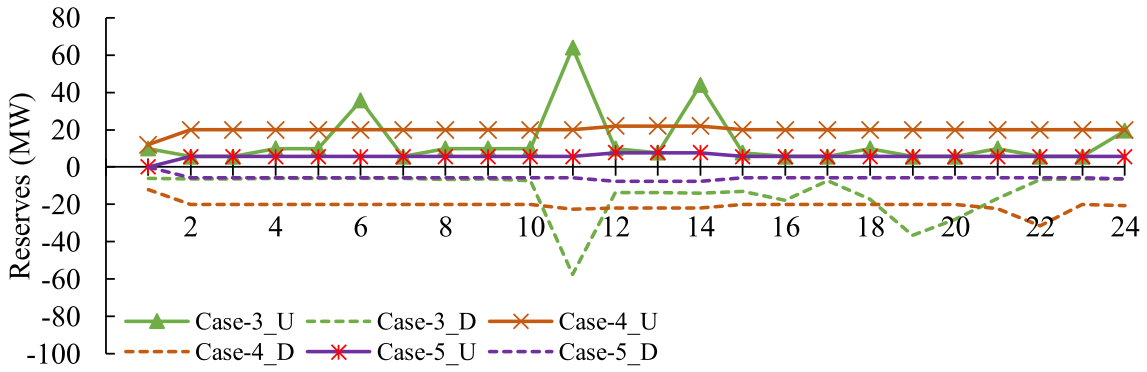

FIGURE 2. Reserves for critical period in different cases.

TABLE 1. Specifications of test cases.

Cases	Reserve cost		CA Features		
	Wind	CA	Critical period	Post-CA	ELR
Case-0	✓	–	–	–	–
Case-1	✓	–	✓	–	–
Case-2	✓	✓	✓	–	–
Case-3	✓	–	✓	✓	✓
Case-4	✓	✓	✓	✓	–
Case-5 (proposed)	✓	✓	✓	✓	✓

$$T_s^{l,B}\Bigg(\sum_{i\in\gamma}\hat{P}_{i,t}^{\delta}+\sum_{m\in\phi}\hat{P}_{m,t}+\sum_{n\in\psi}\hat{P}_{n,t}^{\delta} - Pl_s^t+S_\delta^t\Bigg)\geq Fl_l^{\max}. \tag{77}$$

IV. CASE STUDY-RESULTS AND ANALYSIS

The numerical results of the implementation of the proposed mixed-integer linear problem (MILP) on two test systems are evaluated in this section. The 6-bus and the IEEE 118-bus test systems are analyzed for six defined cases to show the model performance. The six cases, given in Table 1, are defined based on different conditions in the critical and post-contingency periods with and without considering the contingency reserve cost. This is to show their impact on the proposed stochastic SCUC model. The basic model of Case-0 is defined as a stochastic model with wind uncertainties, and the number of scenarios after reduction is five. Cases 1-4 represent the different variation of the stochastic model in Case-0. Case-5 is the comprehensive model which considers all the features presented in this paper. These tests are performed using CPLEX, on a laptop with Intel 7core 2.4 GHz and 8 GB of RAM. The detailed information of the test systems is available online at [28].

A. 6-BUS TEST SYSTEM

The 6-bus test system contains three generators, and one wind farm and two storage units are added to evaluate the proposed model. In this test system, all generators are from the first type with FRSs, and hence, they are capable of providing immediate and stable re-dispatches at contingency events and regulation reserves. The FRSs for stabilizing the frequency through the critical period are deployed for *N-1* CA of all outages in lines of this test system. Figure 2 shows the total values of FRSs for cases 3-5. It can be seen that, without considering the cost of reserves in Case-3, larger values of FRSs are deployed. The reason is that the model only looks for the minimum values for base dispatches, and does not change them further to reduce the values of contingency reserves, which has no cost. As can be seen in Figure 2, this point is considered in our model; consequently, the dispatched energy is less than the values in cases 3 and 4.

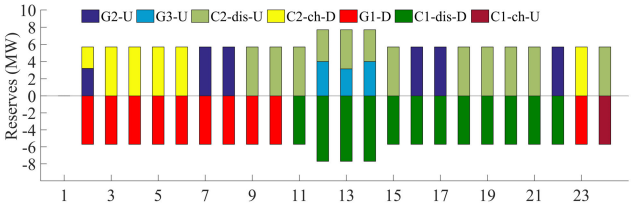

FIGURE 3. Detailed values of reserves for critical period in Case-5.

Figure 3 shows the values of FRSs provided by storage devices, generators with FRSs, and wind farms in Case-5. It can be seen that different types of units participate in providing reserves. Table 2 shows the immediate re-dispatches of the units to evaluate the performance of the FRSs in case of occurrence of contingency events in the different lines in the test network. It can be seen that the storage devices are participating in both charging/discharging modes and in up/down directions.

As mentioned before, the storage devices cannot provide reserve during the post-contingency period as this will affect their state of charge; consequently, this may lead to an infeasible solution. Figure 4 shows the hourly reserves for stable re-dispatches. The larger values of downward reserves are deployed in Case-1 and Case-3 as the cost of contingency reserve has not been considered in these cases. Figure 5 gives the value of reserves provided by different units in Case-5.

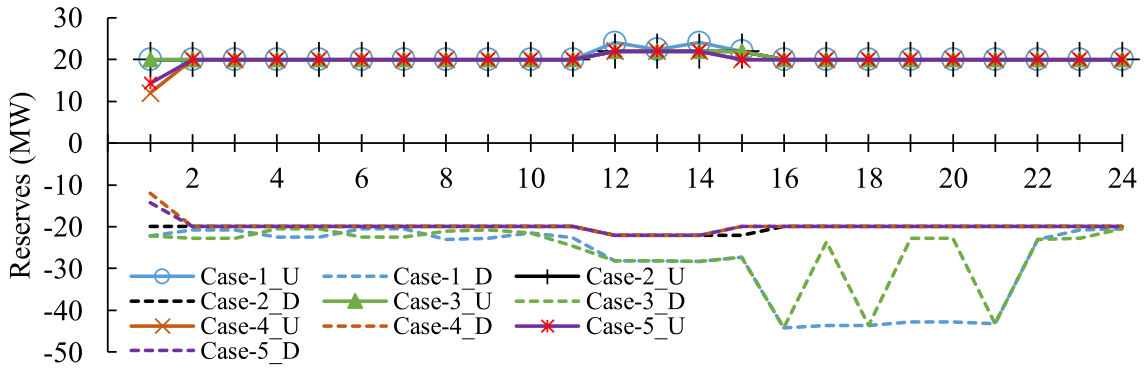

FIGURE 4. Reserves during the post-contingency period in different cases.

TABLE 2. Re-dispatches during critical period and post-contingency (MW).

			Contingencies						
			$l=1$	$l=2$	$l=3$	$l=4$	$l=5$	$l=6$	$l=7$
Critical Period	t13	G_3^U	3.151	3.151	3.151	3.151	3.151	3.151	3.151
	t13	$C_{1,dis}^D$	-7.7	-7.7	-7.7	-7.7	-7.7	-7.7	-7.7
	t13	$C_{2,dis}^U$	4.549	4.549	4.549	4.549	4.549	4.549	4.549
	t21	$C_{1,dis}^D$	-5.7	-5.7	-5.7	-5.7	-5.7	-5.7	-5.7
	t21	$C_{2,dis}^U$	5.7	5.7	5.7	5.7	5.7	5.7	5.7
Post Contingency	t13	G_1^D	-22	-22	-22	0	-22	-18.85	0
	t13	G_2^U	18.85	18.85	18.85	0	18.85	18.85	0
	t13	G_3^U	3.15	3.15	3.15	0	3.15	0	0
	t21	G_1^D	-20	-20	-20	-20	-20	0	-20
	t21	G_2^U	20	20	20	20	20	0	20

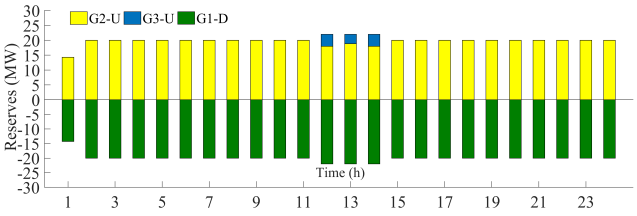

FIGURE 5. Reserves dispatching during the post-contingency in Case-5.

Table 2 also presents the re-dispatches of units for the contingencies in the different network's lines at hour 13 and hour 21. It can be seen that the sum of up/down re-dispatches is zero for each event. This means that the supply is shifted in the post-contingency period to prevent the network overloading or load curtailment.

In this case study, the share of wind energy in the hourly load supply is up to 20%, and the achieved peak-shaving is around 8.41% by using the storage devices and the wind farm.

Figure 6 shows the hourly regulation reserves for Case-5. It can be seen that the highest dispatched values in upward and downward mode happen between hours 12 to 15.

B. IEEE 118-BUS TEST SYSTEM

This test system includes 54 generators. Here, 10 generators of the first type with FRSs are used to provide contingency reserve, and 35 generators of the second type with FRSs are considered as regulation reserve providers. Furthermore, 3 wind farms and 10 storage units are added to this test system. This is to assess the impact of wind and storage units in the suggested model. The IEEE 118-bus test system has 186 lines, and considering the outages of all these lines increases the computing time significantly. Hence, an OCR method is performed to consider only the high impact outages. The method allows consideration of approximately 10% of top-ranked lines. This method is based on the "$ILOI_l^t$" index given by (79). The proposed index uses the power flow of the base case sub-problem and the master solution, in the corresponding iteration, as shown by (78).

$$Fl_l^t = T_s^l\Big(\sum_{i\in\Lambda}\hat{P}_{i,t} + \sum_{m\in\phi}\hat{P}_{m,t} + \sum_{n\in\psi}\sum_{\delta}(\Omega_\delta\hat{P}_{n,t}^\delta) - Pl_s^t\Big) \tag{78}$$

$$ILOI_l^t = (Fl_l^t/Fl_l^{\max})\frac{1}{FOR_l}. \tag{79}$$

To evaluate the deployment of reserves, Figure 7 represents the values of dispatched reserves during the critical period and for different cases 3-5. It can be seen, in Case-3, large values of redundant reserves are deployed in upward and downward modes. Figure 8 shows the values of hourly reserves of different units for Case-5, where generators with FRSs, storage devices, and wind farms participate in the deployment of contingency reserves during the critical period.

Table 3 presents the re-dispatches during the critical period of contingencies at hour 21. It can be seen that downward reserves are supplied by different units in different

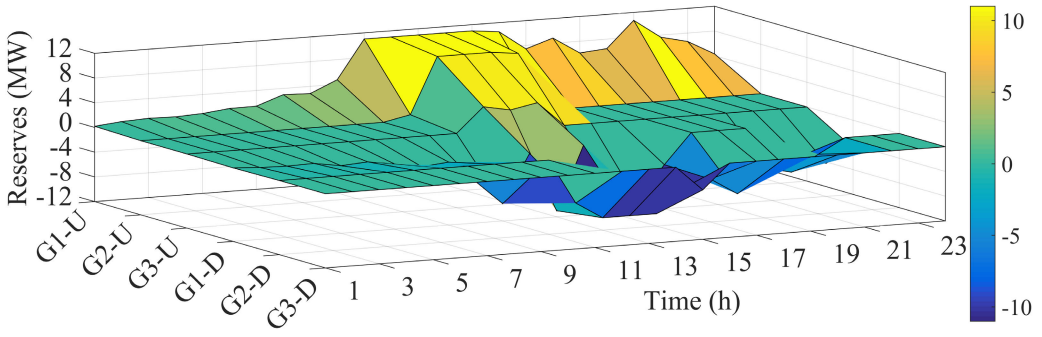

FIGURE 6. Hourly regulation reserve for wind variations in Case-5.

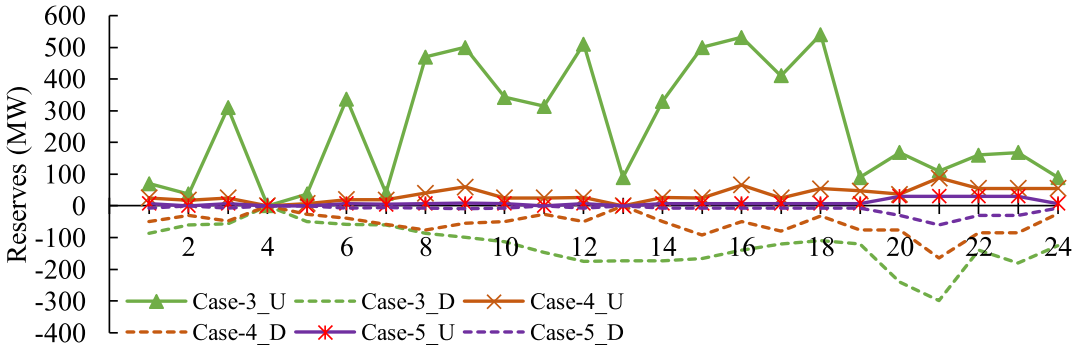

FIGURE 7. Reserves for critical period in different cases.

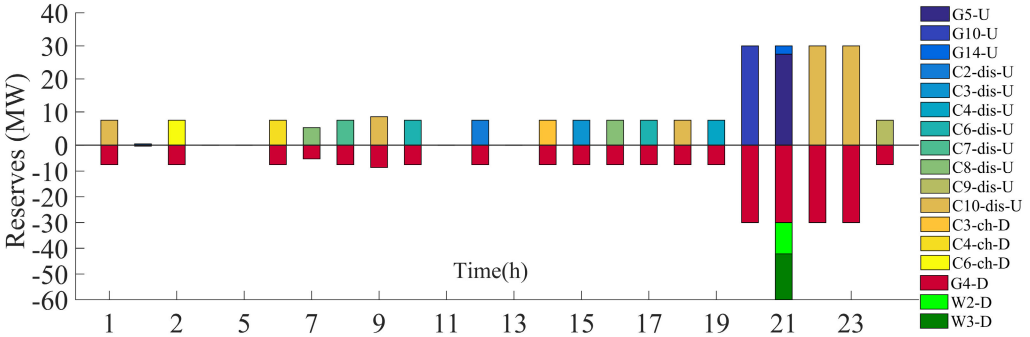

FIGURE 8. Detailed values of critical period reserves in Case-5.

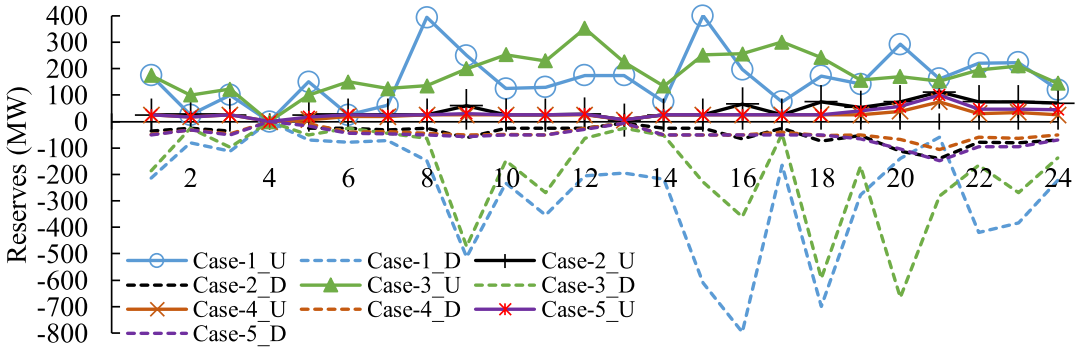

FIGURE 9. Deployed reserves during the post-contingency in different cases.

contingencies, and contingencies are sorted based on the defined ranking index. Besides, the sum of re-dispatches in each contingency is zero. The storage devices mostly deploy upward reserves during the critical period of contingencies.

The deployed values of reserves during the post-contingency period are presented in Figure 9. It can be seen that the reserve deployment in the post-contingency period is significantly affected by considering the cost of reserves.

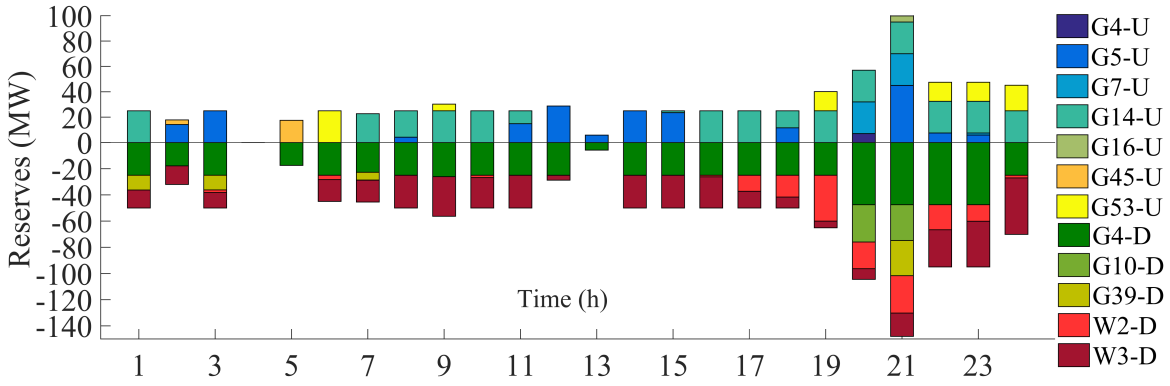

FIGURE 10. Deployed reserves during the post-contingency period for Case-5.

TABLE 3. Re-dispatches during critical period (MW).

	Contingencies								
l	129	29	8	28	74	167	132	61	161
G_5^U	27.5	27.5	27.5	27.5	27.5	27.5	27.5	27.5	27.5
G_{14}^U	2.5	2.5	2.5	0	2.5	2.5	0	2.5	2.5
G_4^D	0	0	-30	0	0	-12.2	0	-12.2	0
W_2^D	-12.2	-12.2	0	-9.7	-12.2	0	-9.7	0	-12.2
W_3^D	-17.8	-17.8	0	-17.8	-17.8	-17.8	-17.8	-17.8	-17.8
l	31	130	41	186	66	67	27	62	59
G_5^U	27.5	27.5	27.5	27.5	27.5	27.5	27.5	27.5	27.5
G_{14}^U	2.5	2.5	0	2.5	2.5	2.5	2.5	2.5	2.5
G_4^D	-12.2	0	0	0	0	0	-12.2	0	0
W_2^D	0	-12.2	-9.7	-12.2	-12.2	-12.2	0	-12.2	-12.2
W_3^D	-17.8	-17.8	-17.8	-17.8	-17.8	-17.8	-17.8	-17.8	-17.8

TABLE 4. Re-dispatches during the post-contingency period (MW).

	Contingencies								
l	129	29	8	28	74	167	132	61	161
G_5^U	0	45	45	0	0	0	0	0	0
G_7^U	0	25	25	5.5	25	25	21.8	25	0
G_{14}^U	25	25	0	25	25	25	25	25	25
G_{16}^U	0	4.8	4.8	0	0	4.8	0	0	2.8
G_{53}^U	0.7	0.7	0	0.7	0	0.7	0.7	0.7	0.7
G_4^D	0	0	-47.5	0	-47.5	-47.5	-47.5	-22.2	0
G_{10}^D	0	-27.3	-27.3	-27.3	-2.5	0	0	0	0
G_{39}^D	0	-26.9	0	0	0	0	0	0	0
W_2^D	-25.7	-28.5	0	-3.9	0	-8	0	-28.5	-28.5
W_3^D	0	-17.8	0	0	0	0	0	0	0
l	31	130	41	186	66	67	27	62	59
G_7^U	0	0	25	25	25	0	2.8	25	0
G_{14}^U	25	25	25	25	25	25	25	17	25
G_{16}^U	4.8	0	0	4.8	0	4.8	0	4.8	2.8
G_{53}^U	0.7	0.7	0.7	0.71	0	0.7	0.7	0.7	0.7
G_4^D	-30.5	-25.7	-47.5	-28.2	-47.5	-2 0	-47.5	0	
G_{10}^D	0	0	0	-27.3	-2.5	0	0	0	0
W_2^D	0	0	-3.2	0	0	-28.5	-28.5	0	-28.5

As mentioned before, the storage devices cannot deploy reserves for a long period, and Figure 10 shows the reserves provided by generators and wind farms in Case-5.

Table 4 shows the stable re-dispatches during the post contingency period at hour 21, and it can be seen the wind farms participate alongside other units in re-dispatches.

Figure 11 presents the hourly regulation reserves for covering the wind power variations. It can be seen the reserves are mostly deployed between hours 16 and 24, where the highest level of wind energy penetration takes place.

A comparison between the operational cost, including the cost of generation and reserves, in different cases, is presented in Table 5. As expected, in Case-2 and Case-5 the total cost is increased, when the cost of contingency reserves is considered. Moreover, considering the ELR in Case-5 decreased the cost in comparison to Case-4. The total costs for Case-5 (the target model of this paper) are \$156679 and \$1740671 for the 6-bus and IEEE 118-bus test systems, respectively.

Table 6 compares the solution time of the proposed model in different cases. It can be obtained that without considering the reserve costs for contingencies, the deployment of redundant reserves makes the convergence slow because of oscillation in the iterative process. Also, the computing time of Case-5, corresponding to the developed model in this paper, without considering the ASP and OCR is 93 seconds and 3742 seconds for the 6-bus and IEEE 118-bus test systems. However, after considering these acceleration

TABLE 5. Cost evaluation (\$).

Cases	Six-bus			IEEE 118-bus		
	Res	Gen	Total	Res	Gen	Total
Case-0	259	136539	136798	5298	1733823	1739121
Case-1	314	154379	154692	5283	1733995	1739277
Case-2	957	155330	156286	6066	1734305	1740370
Case-3	314	154379	154692	5286	1734260	1739545
Case-4	2091	155695	157786	6145	1734950	1741095
Case-5	1241	155438	156679	5978	1734692	1740671

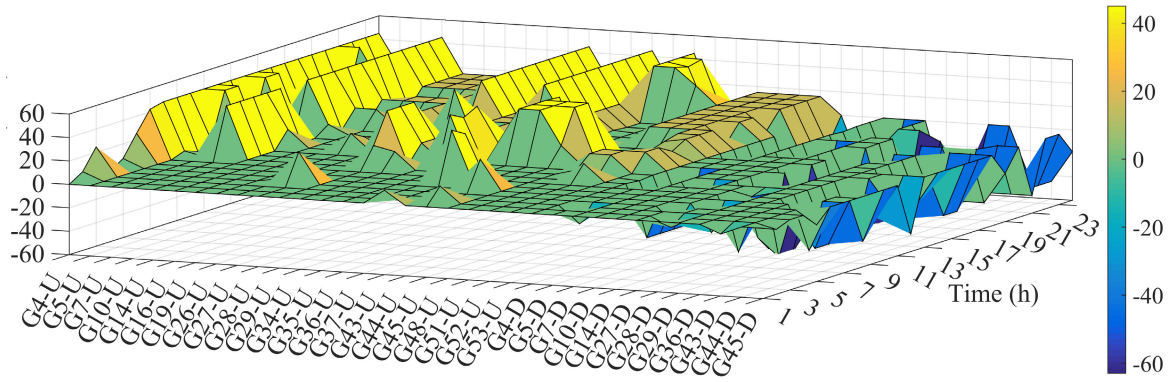

FIGURE 11. Hourly regulation reserve for wind variations in Case-5.

TABLE 6. Solution time evaluation (MIP duality gap = 0).

Cases	Six-bus		IEEE 118-bus	
	Time(sec)	Iterations	Time(sec)	Iterations
Case-0	2	2	52	3
Case-1	4	6	1633	17
Case-2	3	5	1014	11
Case-3	12	13	1553	14
Case-4	8	7	2088	22
Case-5	6	7	1208	16
OCR&ASP=NO	93	11	3742	29

techniques, the computing time becomes 6 seconds and 1208 seconds, respectively.

V. CONCLUSION

This paper presented a stochastic SCUC to schedule the regulation and contingency reserves while considering the fluctuation of wind power, the response time of different facilities as well as contingencies. The model coordinated the performance of generators used as contingency reserves and also used as a regulation reserve to cope with wind variation. The Benders decomposition with two acceleration techniques (based on OCR and ASP) is developed and successfully applied to the model. The following conclusions are obtained based on the evaluation of numerical results:

- The generators with FRSs, storage devices, and wind farms secure the critical period after contingencies and considering the ELR improves the operational cost;
- The FRSs are deployed by storage devices without any violation regarding the base schedule, while it fulfills the re-dispatch schedules in contingencies;
- The re-dispatch schedules of generators and wind farms during the post-contingency period are validated using the *N-1* contingency analysis;
- If the reserve costs are neglected, the model will deploy redundant reserves from different units in all contingency cases. The redundant reserves will impose a significant charge on operators in the market clearing process;
- The reported execution times show the effectiveness of the applied acceleration techniques.

Future research directions include the provision of ancillary services from various types of storage devices (with different response-time) and swappable storage systems that can be used for covering uncertainties of variable energy resources and contingencies.

APPENDIX

$$S_B^t + \sum_l (\mu 1_{l,t}^B - \mu 2_{l,t}^B) T_s^{l,B} \Big[\sum_{i\in\Lambda} (P_{i,t} - \hat{P}_{i,t}) + \sum_{m\in\phi} (P_{m,t} - \hat{P}_{m,t}) + \sum_\delta \Omega_\delta \sum_{n\in\psi} (P_{n,t}^\delta - \hat{P}_{n,t}^\delta) \Big] \le 0 \quad (80)$$

$$S_c^{t,\tau_1} + \sum_i \Big(\mu 1_{i,t}^{c,\tau_1} (P_{i,t} - \hat{P}_{i,t} + R_{i,t}^{1,U} - \hat{R}_{i,t}^{1,U}) - \mu 2_{i,t}^{c,\tau_1} (P_{i,t} - \hat{P}_{i,t} - R_{i,t}^{1,D} + \hat{R}_{i,t}^{1,D}) \Big) + \sum_m \Big(\mu 3_{m,t}^{c,\tau_1} (P_{m,t}^{ch} - \hat{P}_{m,t}^{ch} + R_{m,t}^{ch,U} - \hat{R}_{m,t}^{ch,U}) - \mu 4_{m,t}^{c,\tau_1} (P_{m,t}^{ch} - \hat{P}_{m,t}^{ch} - R_{m,t}^{ch,D} + \hat{R}_{m,t}^{ch,D}) + \mu 5_{m,t}^{c,\tau_1} (P_{m,t}^{dis} - \hat{P}_{m,t}^{dis} + R_{m,t}^{dis,U} - \hat{R}_{m,t}^{dis,U}) - \mu 6_{m,t}^{c,\tau_1} (P_{m,t}^{dis} - \hat{P}_{m,t}^{dis} - R_{m,t}^{dis,D} + \hat{R}_{m,t}^{dis,D}) \Big) + \sum_n \Big(\mu 7_{n,t}^{c,\tau_1} \Big(\sum_\delta \Omega_\delta (P_{n,t}^\delta - \hat{P}_{n,t}^\delta) \Big) - \mu 8_{n,t}^{c,\tau_1} \Big(\sum_\delta \Omega_\delta (P_{n,t}^\delta - \hat{P}_{n,t}^\delta) - R_{n,t}^{1,D} + \hat{R}_{n,t}^{1,D} \Big) \Big) \le 0 \quad (81)$$

$$S_c^{t,\tau_2} + \sum_i \Big(\mu 1_{i,t}^{c,\tau_2} (P_{i,t} - \hat{P}_{i,t} + R_{i,t}^{2,U} - \hat{R}_{i,t}^{2,U}) - \mu 2_{i,t}^{c,\tau_2} (P_{i,t} - \hat{P}_{i,t} - R_{i,t}^{2,D} + \hat{R}_{i,t}^{2,D}) \Big) + \sum_n \Big(\mu 3_{n,t}^{c,\tau_2} \sum_\delta \Omega_\delta (P_{n,t}^\delta - \hat{P}_{n,t}^\delta) - \mu 4_{n,t}^{c,\tau_2} \times \Big(\sum_\delta \Omega_\delta (P_{n,t}^\delta - \hat{P}_{n,t}^\delta) - R_{n,t}^{2,D} + \hat{R}_{n,t}^{2,D} \Big) \Big) + \sum_l \Big((\mu 5_{l,t}^{c,\tau_2} - \mu 6_{l,t}^{c,\tau_2}) \times T_s^{l,c} \sum_{m\in\phi(s)} (P_{m,t} - \hat{P}_{m,t}) \Big) - \sum_m \Big(\mu 7_t^{c,\tau_2} (P_{m,t} - \hat{P}_{m,t}) \Big) \le 0 \quad (82)$$

$$S^t_\delta + \sum_l (\mu 1^\delta_{l,t} - \mu 2^\delta_{l,t}) T^{l,B}_s \Big[\sum_{i\in\Lambda} (P^\delta_{i,t} - \hat{P}^\delta_{i,t}) + \sum_{m\in\phi} (P_{m,t} - \hat{P}_{m,t}) + \sum_{n\in\psi} (P^\delta_{n,t} - \hat{P}^\delta_{n,t}) \Big] \le 0. \quad (83)$$

REFERENCES

[1] M. Habibi, V. Vahidinasab, A. Pirayesh, M. Shafie-khah, and J. P. S. Catalao, "An enhanced contingency-based model for joint energy and reserve markets operation by considering wind and energy storage systems," *IEEE Trans. Ind. Informat.*, early access, Jul. 14, 2020, doi: 10.1109/TII.2020.3009105.

[2] M. Habibi, V. Vahidinasab, J. Aghaei, and B. Mohammadi-Ivatloo, "Assessment of energy storage systems as a reserve provider in stochastic network constrained unit commitment," *IET Smart Grid*, Jan. 2021, doi: 10.1049/stg2.12012.

[3] National Grid Electricity System Operator (ESO). *Interim Report Into the Low Frequency Demand Disconnection (LFDD) Following Generator Trips and Frequency Excursion*. Accessed: Aug. 9, 2019. [Online]. Available: https://www.nationalgrideso.com/document/151081/download

[4] M. Habibi, V. Vahidinasab, A. Allahham, D. Giaouris, S. Walker, and P. Taylor, "Coordinated storage and flexible loads as a network service provider: A resilience-oriented paradigm," in *Proc. IEEE 28th Int. Symp. Ind. Electron. (ISIE)*, Jun. 2019, pp. 58–63.

[5] National Grid Electricity System Operator (ESO). *Technical Report on the Events*. Accessed: Aug. 9, 2019. [Online]. Available: https://www.ofgem.gov.uk/system/files/docs/2019/09/eso_technical_report_-_final.pdf

[6] V. Vahidinasab and M. Habibi, *Electric Energy Storage Systems Integration in Energy Markets and Balancing Services*, 1st ed. Amsterdam, The Netherlands: Elsevier, 2021, ch. 15.

[7] National Grid Electricity System Operator (ESO). (Sep. 9, 2019). *Balancing Services*. Accessed: Aug. 9, 2019. [Online]. Available: https://www.nationalgrideso.com/balancing-services

[8] M. Habibi and V. Vahidinasab, "Emergency services of energy storage systems for wind ramp events," in *Proc. Smart Grid Conf. (SGC)*, Dec. 2019, pp. 1–6.

[9] H. Quan, D. Srinivasan, and A. Khosravi, "Integration of renewable generation uncertainties into stochastic unit commitment considering reserve and risk: A comparative study," *Energy*, vol. 103, pp. 735–745, May 2016.

[10] M. Habibi, V. Vahidinasab, and M. S. Sepasian, "Application of mobile energy storage to facilitate energy transfer between TSO and DSO networks," in *Proc. 10th Smart Grid Conf.*, Dec. 2020, pp. 1–6.

[11] M. Habibi, A. Oshnoei, V. Vahidinasab, and S. Oshnoei, "Allocation and sizing of energy storage system considering wind uncertainty: An approach based on stochastic SCUC," in *Proc. Smart Grid Conf. (SGC)*, Nov. 2018, pp. 1–6.

[12] S. M. Hashemi, V. Vahidinasab, M. S. Ghazizadeh, and J. Aghaei, "Valuing consumer participation in security enhancement of microgrids," *IET Gener., Transmiss. Distrib.*, vol. 13, no. 5, pp. 595–602, Mar. 2019.

[13] A. Khodaei, M. Shahidehpour, and S. Bahramirad, "SCUC with hourly demand response considering intertemporal load characteristics," *IEEE Trans. Smart Grid*, vol. 2, no. 2, pp. 564–571, Sep. 2011.

[14] Q. Wang, J.-P. Watson, and Y. Guan, "Two-stage robust optimization for N-K contingency-constrained unit commitment," *IEEE Trans. Power Syst.*, vol. 28, no. 3, pp. 2366–2375, Aug. 2013.

[15] P. Panciatici, Y. Hassaine, S. Fliscounakis, L. Platbrood, M. Ortega-Vazquez, J. L. Martinez-Ramos, and L. Wehenkel, "Security management under uncertainty: From day-ahead planning to intraday operation," in *Proc. IREP Symp. Bulk Power Syst. Dyn. Control (IREP)*, Aug. 2010, pp. 1–8.

[16] A. Nikoobakht, J. Aghaei, M. Mardaneh, T. Niknam, and V. Vahidinasab, "Moving beyond the optimal transmission switching: Stochastic linearised SCUC for the integration of wind power generation and equipment failures uncertainties," *IET Gener., Transmiss. Distrib.*, vol. 12, no. 15, pp. 3780–3792, Aug. 2018.

[17] Y. Wen, C. Guo, H. Pandzic, and D. S. Kirschen, "Enhanced security-constrained unit commitment with emerging utility-scale energy storage," *IEEE Trans. Power Syst.*, vol. 31, no. 1, pp. 652–662, Jan. 2016.

[18] J. Wang, M. Shahidehpour, and Z. Li, "Contingency-constrained reserve requirements in joint energy and ancillary services auction," *IEEE Trans. Power Syst.*, vol. 24, no. 3, pp. 1457–1468, Aug. 2009.

[19] M. Habibi, V. Vahidinasab, A. Allahham, D. Giaouris, H. Patsios, and P. Taylor, "Exploitation of ancillary service from energy storage systems as operational reserve," in *Proc. UK Energy Storage Conf.* Newcastle upon Tyne, U.K.: Newcastle Univ., 2019, p. 1.

[20] Q. Zhai, X. Li, X. Lei, and X. Guan, "Transmission constrained UC with wind power: An all-scenario-feasible MILP formulation with strong nonanticipativity," *IEEE Trans. Power Syst.*, vol. 32, no. 3, pp. 1805–1817, May 2017.

[21] X. Wang, Z. Li, M. Shahidehpour, and C. Jiang, "Robust line hardening strategies for improving the resilience of distribution systems with variable renewable resources," *IEEE Trans. Sustain. Energy*, vol. 10, no. 1, pp. 386–395, Jan. 2019.

[22] M. I. Alizadeh, M. P. Moghaddam, and N. Amjady, "Multistage multiresolution robust unit commitment with nondeterministic flexible ramp considering load and wind variabilities," *IEEE Trans. Sustain. Energy*, vol. 9, no. 2, pp. 872–883, Apr. 2018.

[23] C. Sahin, M. Shahidehpour, and I. Erkmen, "Allocation of hourly reserve versus demand response for security-constrained scheduling of stochastic wind energy," *IEEE Trans. Sustain. Energy*, vol. 4, no. 1, pp. 219–228, Jan. 2013.

[24] J. Aghaei, M. Karami, K. M. Muttaqi, H. A. Shayanfar, and A. Ahmadi, "MIP-based stochastic security-constrained daily hydrothermal generation scheduling," *IEEE Syst. J.*, vol. 9, no. 2, pp. 615–628, Jun. 2015.

[25] The Weather Company. (2019). *Hourbyhour Prediction of Wind Speed*. [Online]. Available: https://weather.com/weather/hourbyhour

[26] A. J. Conejo, M. Carrión, and J. M. Morales, *Decision Making Under Uncertainty in Electricity Markets*, vol. 1. New York, NY, USA: Springer, 2010.

[27] L. Wu, M. Shahidehpour, and Z. Li, "Comparison of scenario-based and interval optimization approaches to stochastic SCUC," *IEEE Trans. Power Syst.*, vol. 27, no. 2, pp. 913–921, May 2012.

[28] *Input Data: The 6-Bus and IEEE 118-Bus Test Systems*. Accessed: Nov. 20, 2020. [Online]. Available: http://www.vahidinasab.com/data/FRS.zip

MAHDI HABIBI received the B.Sc. degree from the Babol Noshirvani University of Technology, Babol, Iran, in 2014, and the M.Sc. degree from the Shahid Beheshti University of Technology (SBU), Tehran, Iran, in 2016, both in electrical engineering, where he is currently pursuing the Ph.D. degree in power system electrical engineering.

His research interests include the power system operation, system management under uncertainty, integration of renewable energy resources, provision of flexibility services, scheduling storage devices, and optimization models at transmission and distribution levels. He is a member of the SOHA Smart Energy Systems Laboratory, SBU.

VAHID VAHIDINASAB (Senior Member, IEEE) received the Ph.D. degree (Hons.) in electrical engineering from the Iran University of Science and Technology, Tehran, Iran, in 2010.

Since 2010, he has been with the Department of Electrical Engineering, Shahid Beheshti University (SBU), as an Assistant Professor. He has also founded and managed the SOHA Smart Energy Systems Laboratory, SBU. He has demonstrated a consistent track record of attracting external funds and managed industrial projects and closely worked with a number of large and complex national/international projects. From 2011 to 2018, he held a number of leadership roles at SBU and the Niroo Research Institute. In 2018, he moved to Newcastle University, where he is currently a Senior Research Associate and manages the inteGRIDy as an EU Horizon 2020 Project. He also works with the EPSRC Active Building Centre (ABC). His work is funded by the U.K.-EPSRC, EU-H2020, and industry partners and local utilities of Iran and the U.K.

Dr. Vahidinasab is a member of the IEEE Power and Energy Society (PES) and the IEEE Smart Grid Community. He is also a member of the Editorial Board and a Subject Editor of the *IET Generation, Transmission & Distribution* and an Associate Editor of the *IET Smart Grid* and IEEE Access. He is also the Guest Editor-in-Chief of the Special Issue on "Power and Energy Systems Operation in Time of Pandemics: Lessons Learned from COVID-19 Lockdown" of the *International Journal of Electrical Power & Energy Systems*. He was considered as one of the outstanding reviewers of the IEEE Transactions on Sustainable Energy, in 2018, and the IEEE Transactions on Power Systems, in 2020.

MOHAMMAD SADEGH SEPASIAN received the B.Sc. degree in electrical engineering from Tabriz University, Tabriz, Iran, in 1990, and the M.Sc. degree in electrical engineering from Tehran University, Tehran, Iran, in 1993, and the Ph.D. degree in electrical engineering from Tarbiat Modares University, Tehran, in 1999.

He is currently an Associate Professor with the Department of Electrical Engineering, Shahid Beheshti University, Tehran. His research interests include power system planning, distribution system issues, and application of artificial intelligence and optimization methods in power system studies.

ADIB ALLAHHAM received the B.S. degree in electric engineering from Damascus University, Syria, and the M.Sc. and Ph.D. degrees from the Joseph Fourier University of Grenoble, France, in 2004 and 2008, respectively. From 1999 to 2003, he worked at the energy industry. In 2008, he joined the G-SCOP Laboratory, France, as a Postdoctoral Researcher. From 2009 to June 2016, he worked as a Senior Lecturer with the Electrical Power Engineering Department, Damascus University. Since 2016, he has been a Researcher with the School of Engineering, Newcastle University. He has published more than 20 peer-reviewed journal and international conference papers. His research interests include the energy storage systems, smart grid technologies, grid connected renewable energy sources, and multi-vector energy integration.

DAMIAN GIAOURIS received the B.Eng. degree in automation engineering from the Technological Educational Institute of Thessaloniki, Thessaloniki, Greece, in 2000, the B.Sc. and master's degrees in mathematics from Open University, Milton Keynes, U.K., in 2009 and 2011, respectively, and the M.Sc. and Ph.D. degrees in control of electrical systems from Newcastle University, Newcastle upon Tyne, U.K., in 2001 and 2004, respectively. Since 2004, he has been a Lecturer in control systems with Newcastle University, before moving to the Centre for Research and Technology Hellas, Greece. Since September 2015, he has been a Senior Lecturer in control of electrical systems with Newcastle University. His research interests include control of power converters, power systems, smart grids, electric vehicles, and nonlinear dynamics of electrical systems. He has been an Associate Editor of *IET Power Electronics* and a Guest Associate Editor of the IEEE JOURNAL ON EMERGING AND SELECTED TOPICS IN CIRCUITS AND SYSTEMS. He is also an Associate Editor of IEEE CAS II.

PHIL TAYLOR (Senior Member, IEEE) received the Ph.D. (Eng.) degree in intelligent demand side management techniques from the University of Manchester Institute of Science and Technology (UMIST), Manchester, U.K., in 2001. He previously held the DONG Energy Chair in Renewable Energy and was the Director of the Durham Energy Institute. He joined Newcastle University, Newcastle upon Tyne, U.K., in April 2013, where he was the Head of the School of Engineering and held the Siemens Chair of Energy Systems. He joined the University of Bristol in July 2020, where he is the Pro Vice-Chancellor for Research and Enterprise. He is currently a Visiting Professor at Nanyang Technological University, Singapore.

JAMSHID AGHAEI (Senior Member, IEEE) received the B.Sc. degree in electrical engineering from the Power and Water Institute of Technology, Tehran, Iran, in 2003, and the M.Sc. and Ph.D. degrees from the Iran University of Science and Technology, Tehran, in 2005 and 2009, respectively. He is currently a Full Professor with the Lappeenranta University of Technology (LUT), Lappeenranta, Finland. His research interests include smart grids, renewable energy systems, electricity markets, and power system operation, optimization, and planning. He was a Guest Editor for the Special Section on "Industrial and Commercial Demand Response" of the IEEE TRANSACTIONS ON INDUSTRIAL INFORMATICS, published in November 2018, and the Special Issue on "Demand Side Management and Market Design for Renewable Energy Support and Integration" of the *IET Renewable Power Generation*, published in April 2019. He is an Associate Editor of the IEEE TRANSACTIONS ON SMART GRID, IEEE SYSTEMS JOURNAL, IEEE TRANSACTIONS ON CLOUD COMPUTING, IEEE OPEN ACCESS JOURNAL OF POWER AND ENERGY, and *IET Renewable Power Generation* and a Subject Editor of the *IET Generation Transmission and Distribution*. He was considered one of the outstanding reviewers of the IEEE TRANSACTIONS ON SUSTAINABLE ENERGY, in 2017.